ELSEVIER

Ceramics International 33 (2007) 263–268

CERAMICS INTERNATIONAL

www.elsevier.com/locate/ceramint

Influence of the sintering temperature on phase development in PMnN–PZT ceramics

Chih-Yen Chen, Yi Hu *, Hur-Lon Lin, Wan-Yi Wei

Department of Materials Engineering, Tatung University, Taipei, Taiwan

Received 4 March 2005; received in revised form 6 July 2005; accepted 8 September 2005
Available online 6 January 2006

Abstract

$0.07Pb(Mn_{1/3}Nb_{2/3})O_3$–$0.468PbZrO_3$–$0.462PbTiO_3$ ceramics were prepared by the conventional mixed oxide route and the influence of sintering temperature on their characteristics was studied. Crystal phases were characterized in the coexistence region of the tetragonal and rhombohedral phases, which has been found to occur within the sintering temperature range 1050–1250 °C. The cell parameters a_T and c_T of the tetragonal phase decreased, whereas the parameter a_R of the rhombohedral phase increased as the sintering temperature increased in the phase coexistence region. The relative amount of the rhombohedral phase decreased as the sintering temperature increased. The relationships between microstructure, mechanical quality factor (Q_m), and electromechanical coupling factor (k_p) are discussed.

Keywords: A. Sintering; C. Piezoelectric properties; D. PZT

1. Introduction

The lead zirconate–lead titanate system $Pb(Zr_x–Ti_{1-x})O_3$ (PZT) has excellent piezoelectric properties and high dielectric properties, and has emerged as one of the most widely studied and developed ferroelectric oxides [1–4]. The electromechanical responses of these materials are to be most pronounced at the morphotropic phase boundary (MPB) of the tetragonal and rhombohedral coexistence phases [5–7]. However, the piezoelectric characteristics of the PZT ceramics are very sensitive to preparation methods, compositions, and kinds of additives. Many aliovalent additives have been widely investigated to optimize the critical properties of PZT ceramics [8–12]. Either higher valence substitutions (such as Nb^{5+} and W^{6+}) or lower valence substitutions (such as Mg^{2+} and La^{3+}) can promote their properties. In addition, ''combined substitutions'' with two or more elements have proved to lead to even better properties [3,13]. In our previous work, we used manganese and niobium as combined substitutions resulting in materials which showed good piezoelectric properties in the coexistence region of tetragonal and rhombohedral phases [14]. Compositional fluctuations are believed to be responsible for the coexistence of the two phases and are concerned in the sintering process. This paper discusses the influence of sintering temperature on PZT materials synthesized by the conventional mixed oxide route and especially the phase transition in the coexistence region of the tetragonal and rhombohedral phases.

2. Experimental procedures

$0.07Pb(Mn_{1/3}Nb_{2/3})O_3$–$0.468PbZrO_3$–$0.462PbTiO_3$ (PMnN–PZT) ceramics have been prepared from reagent grade chemicals. First, the columbite phase of manganese niobate ($MnNb_2O_6$) was prepared by calcining the mixture of MnO and Nb_3O_5 at 1100 °C for 2 h. Then the columbite phase was mixed with the appropriate amounts of PbO, TiO_2, and ZrO_2 and calcined at 850C for 2 h. In order to compensate for the evaporation of PbO during sintering, 2 wt.% of excessive PbO was added to the composition. The powders were pressed into 17 mm in diameter and 1.5 mm thick pellets under 122.58 Mpa, which were sintered at various temperatures from 1000 to 1300 °C for 3 h in lead-protected atmosphere. After sintering, the surfaces of the pellets were polished and electrodes were painted with silver-based glue and fired at 590 °C for 12 min. The samples were poled in silicone oil at 120 °C for 30 min under a static electrical field of 4 kV/mm.

* Corresponding author. Tel.: +886 2 25925252; fax: +886 2 25936897.
E-mail address: huyi@ttu.edu.tw (Y. Hu).

0272-8842/$32.00 © 2005 Published by Elsevier Ltd and Techna Group S.r.l.
doi:10.1016/j.ceramint.2005.09.013

The crystallographic structure of the samples was examined by powder X-ray diffraction (XRD) with Cu Kα radiation. The density of the sintered samples was measured with the Archimedes' method. The microstructures of the fractured surface were examined by scanning electron microscopy (SEM). The mechanical quality factor (Q_m) and electromechanical coupling factor (k_p) of the samples were measured using HP 4194A impedance analyzer.

3. Results and discussion

Fig. 1 shows the XRD patterns of the samples sintered at various temperatures. It was found that the predominated phase of the sample sintered at 1100 °C was the rhombohedral ferroelectric phase. However, the rhombohedral phase transformed to the perovskite phase gradually with the increase of the sintering temperature. No rhombohedral phase was observed in samples sintered at $T > 1300$ °C. This was evidenced form the split of the reflection peaks (1 0 0), (2 0 0), and (2 1 0) in the XRD patterns. To analyze the coexistence of the ferroelectric phases, (2 0 0) reflections were chosen because of a higher intensity.

Fig. 2 shows the reflection peaks of the tetragonal phase to shift to a higher angle with the increase of the sintering temperature indicating shrinkage of the cell.

Fig. 3 shows the variation in the lattice parameters of the rhombohedral and tetragonal phases, which were determined from the XRD patterns by the extrapolating method from Nelson–Riky plot. The parameters a_T and c_T of the tetragonal phase decreased, whereas the parameter a_R of the rhombohedral phase increased as the sintering temperature increased in the coexistence region. It has been reported in the literature that splitting of these reflections into triplets occurs in conventionally prepared ceramics due to compositional fluctuations, which derive from diffusion, with manganese and niobium ions of $Pb(Mn_{1/3}Nb_{2/3})O_3$ occupying the same positions of zirconium and titanium ions in $Pb(Zr_{0.503}Ti_{0.497})O_3$ [15]. The radius of the bivalent (2+) manganese ion is much larger than that of Zr^{4+} and Ti^{4+} ions. The substitution of Zr^{4+} or Ti^{4+} ions with Mn^{2+} would cause a large increase in the lattice parameter of the rhombohedral PZT and this is in good agreement with the experimental results as shown in Fig. 3. The substitution of Zr^{4+} or Ti^{4+} ions with Mn^{2+} would cause a distortion of the lattice to make the diffusion of ions more difficult by ''stuffing effect'' and, therefore, slows down the transition from rhombohedral to tetragonal phase.

On the other hand, adding niobium ion has been reported to promote the rhombohedral–tetragonal phase transition [11]. Nb^{5+} is considered as a donor dopant for PZT ceramics, since it substitutes Ti^{4+}/Zr^{4+} ions. Vacancies in A and/or B sites in the perovskite structure would be created due to the charge compensation with the addition of Nb^{5+}. It can be observed that the intensity of the $(0\,0\,2)_T$ reflections increased whereas the $(2\,0\,0)_T$ reflections decreased in the XRD patterns shown in Fig. 2. Therefore, it is thought that the vacancies would occur in

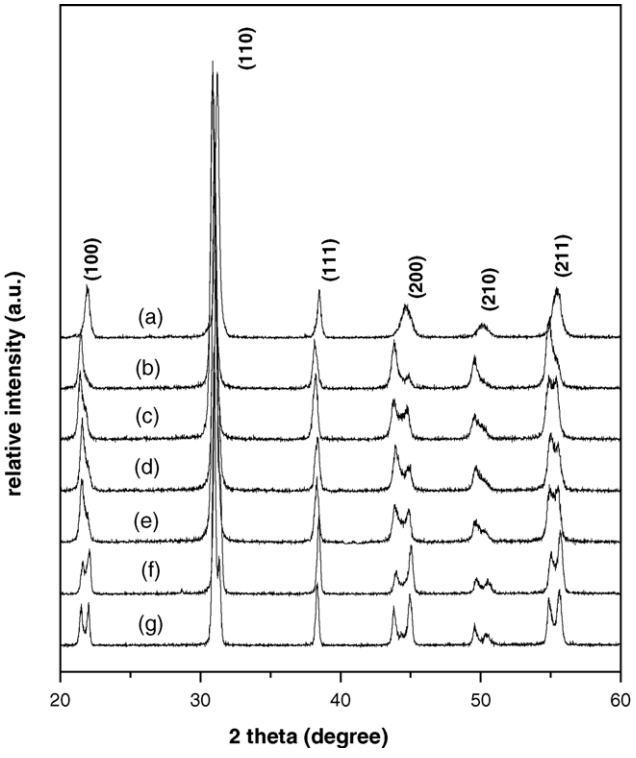

Fig. 1. XRD patterns for PMnN–PZT samples sintered at (a) 1000 °C, (b) 1050 °C, (c) 1100 °C, (d) 1150 °C, (e) 1200 °C, (f) 1250 °C, and (g) 1300 °C for 3 h.

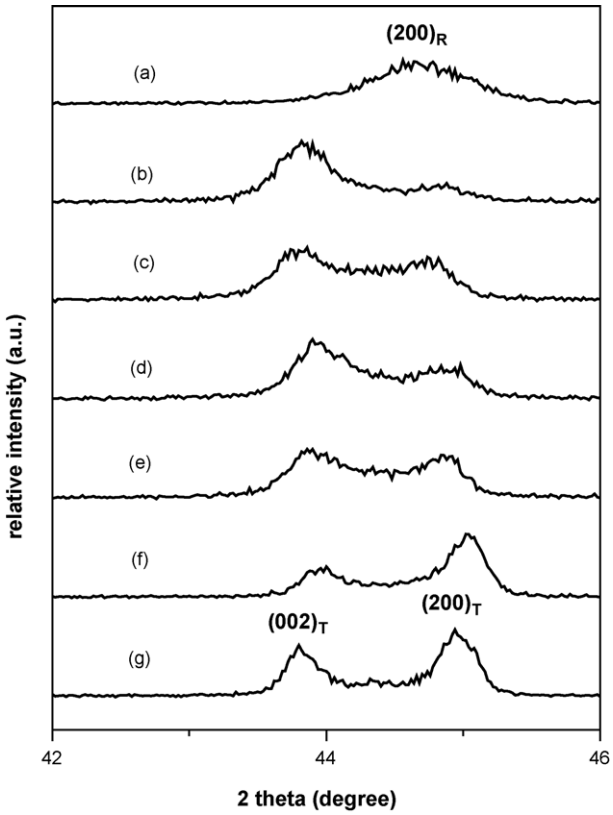

Fig. 2. Profile of the diffraction lines $(0\,0\,2)_T$, $(2\,0\,0)_R$, and $(2\,0\,0)_T$ for PMnN–PZT samples sintered at (a) 1000 °C, (b) 1050 °C, (c) 1100 °C, (d) 1150 °C, (e) 1200 °C, (f) 1250 °C, and (g) 1300 °C for 3 h. The reflections marked R are assigned to rhombohedral phase, whereas those with T are assigned to tetragonal phase.

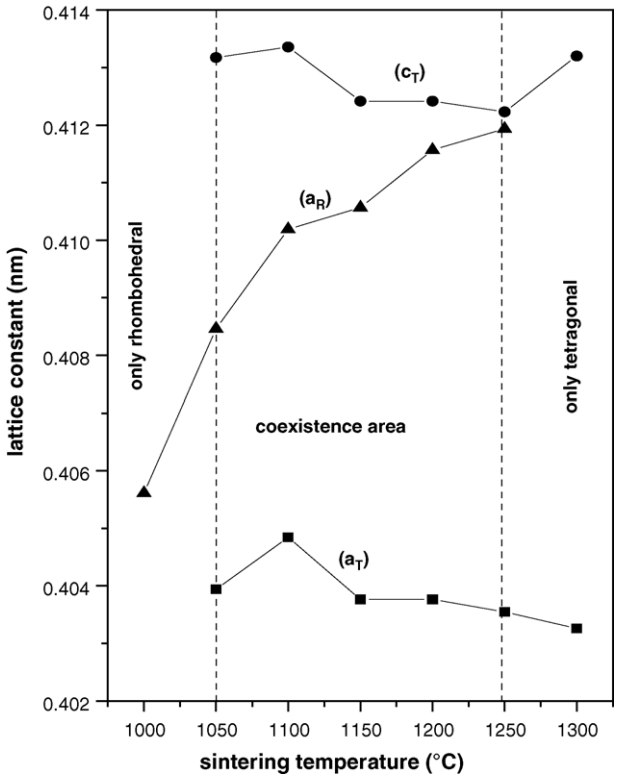

Fig. 3. Variation of lattice parameter for both coexisting ferroelectric phases as a function of sintering temperature.

the A sites which has larger effect on variation of c_T. It has been proposed that the formation of the vacancies at the A site can be expressed as: $Pb(V''_{Pb})_{x/2}(Zr_{0.503}Ti_{0.497}Nb_x)O_3$ [11]. The formation of lead vacancies (V''_{Pb}) would thus cause a decrease in the c_T as shown in Fig. 3. Since the radius of Nb^{5+} is smaller than the average radius of Zr^{4+} and Ti^{4+} (in Table 1), the addition of Nb^{5+} would also cause a decrease in the a_T.

Therefore, the overall reaction sequences observed from the XRD analysis can be represented by the following equations:

$$MnNb_2O_6 + PbO + ZrO_2 + TiO_2 \rightarrow 7\,\text{mol\%}Pb(Mn_{1/3}Nb_{2/3})O_3 + 46.8\%PbZrO_3 + 46.2\%PbTiO_3$$

$$MnNb_2O_6 + PbO + ZrO_2 + TiO_2 \rightarrow 7\%\,Pb(Mn_{1/3}Nb_{2/3})O_3 + Pb(Zr_{0.503}Ti_{0.497})O_3\ (\text{rhombohedral}) \quad T < 1100\,^\circ\text{C}$$

$$MnNb_2O_6 + PbO + ZrO_2 + TiO_2 \rightarrow \text{Mn-rich PZT (rhombohedral)} + \text{Nb-rich PZT(tetragonal)} \quad 1100\,^\circ\text{C} \le T \le 1300\,^\circ\text{C}$$

$$MnNb_2O_6 + PbO + ZrO_2 + TiO_2 \rightarrow Pb(Ti, Mn)(Nb, Zr)O_3\ (\text{tetragonal}) \quad T > 1300\,^\circ\text{C}$$

Fig. 4 shows the relative amount of rhombohedral phase in the phase coexistence region obtained from the XRD patterns.

Table 1
The radius of the cations with coordination number of 6 [18]

Elements	Valence	Radius (Å)
Mn	2+	0.82
	3+	0.65
Zr	4+	0.72
Ti	4+	0.605
Nb	5+	0.64

The relative amount of the rhombohedral phase is approximately calculated from reflection intensities of the triplets as [12]

$$\eta = \frac{I_{(200)R}}{(I_{(200)R} + I_{(200)T} + I_{(002)T})} \quad (1)$$

where $I_{(2\,0\,0)T}$ and $I_{(0\,0\,2)T}$ are the intensities of the (2 0 0) and (0 0 2) reflection lines of the tetragonal phase, respectively, and $I_{(2\,0\,0)R}$ is that of (2 0 0) reflection line of the rhombohedral phase. The integrated intensity was calculated after correcting for instrumental and wavelength related broadening. The relative amount of the rhombohedral phase decreased as the sintering temperature increased. The variation of the lattice parameters and the relative amount of each phase as a function of sintering temperature could be explained by the homogenization of the composition with the enhancement of the diffusion process.

Fig. 5 shows SEM microstructures of the fracture surfaces of samples sintered at various temperatures. The distributions in the grain shape and size of the samples are rather uniform. All the samples showed an intergranular fracture mechanism

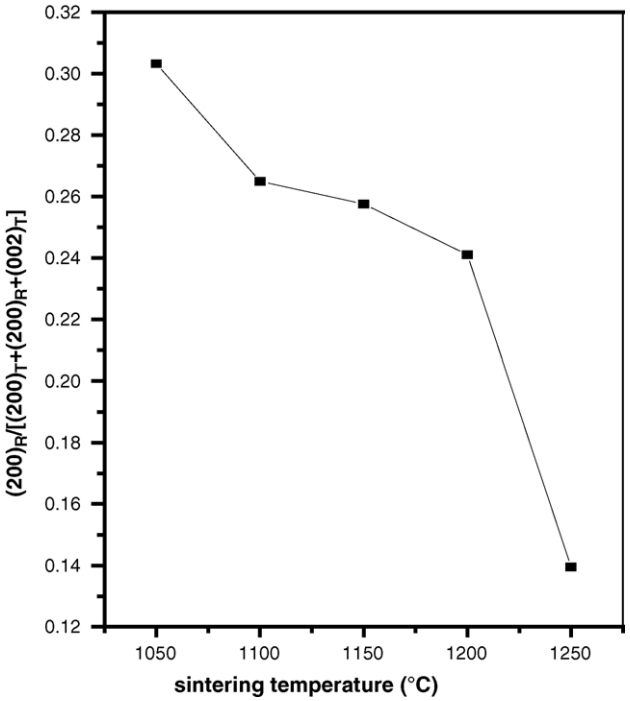

Fig. 4. Relative amount of the rhombohedral phase in the samples versus sintering temperature.

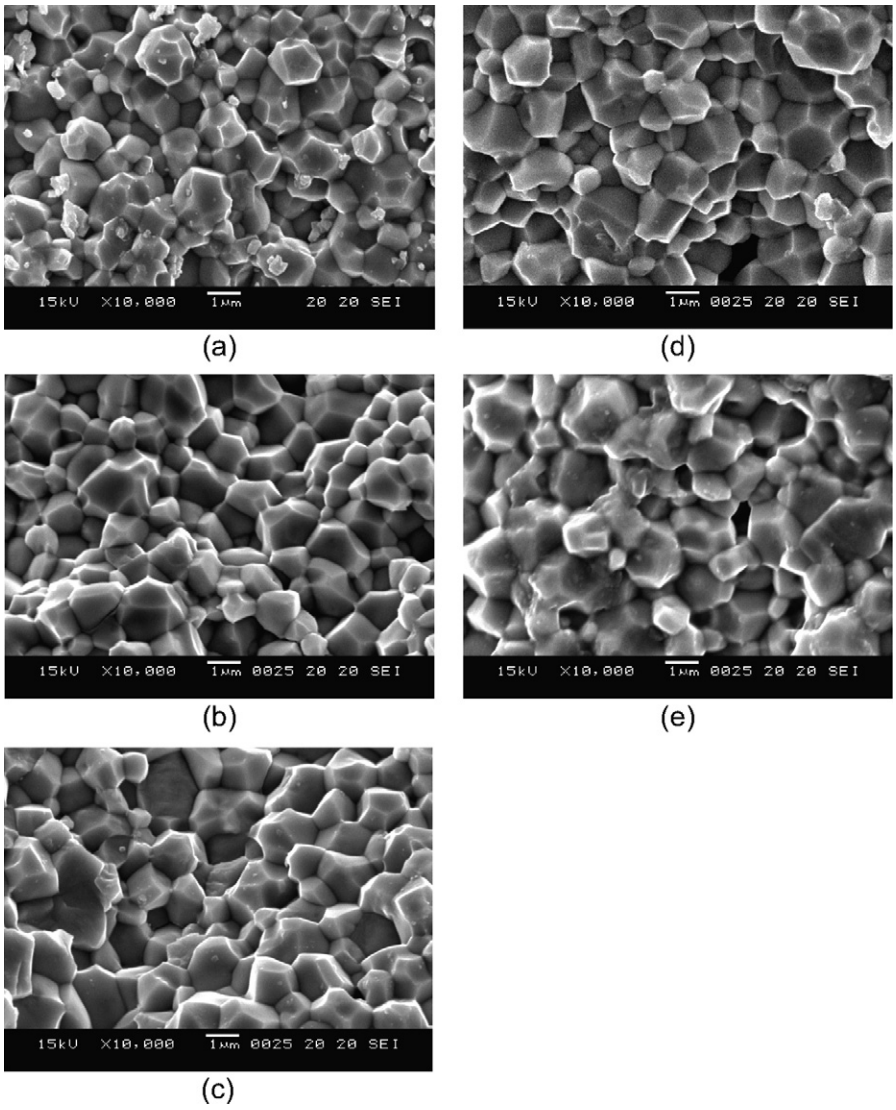

Fig. 5. SEM micrographs of fractured PMnN–PZT ceramics sintered at (a) 1050 °C, (b) 1100 °C, (c) 1150 °C, (d) 1200 °C, and (e) 1250 °C for 3 h.

indicating that the grain boundaries are mechanically weaker than the grains. These samples appear very dense, no pores being evidenced on SEM microstructures.

Fig. 6 shows the relative density (i.e. the measured density divided by the theoretical density of PZT of 8.0 g/cm^3.) of the samples versus sintering temperature. The density of the sample increased largely at sintering temperature higher than 1150 °C and then the rate of densification slows down. This indicates that the diffusion of the cations is enhanced above 1150 °C. Fig. 7 shows the average grain size of the samples versus sintering temperature. The average grain size increased with the increase of the sintering temperature.

The mechanical quality factor, Q_m, of the sample increased as the sintering temperatures increased in the coexistence region (Fig. 8). It was found that samples containing a large amount of rhombohedral phase exhibit lower Q_m values. This can be explained by their lower relative density and smaller grain size, since the smaller grain size with larger interfacial area would increase the friction between domains and thus lowers Q_m value.

Fig. 9 shows the electromechanical planar coupling factor (k_p) versus sintering temperature. Larger k_p factor values have been observed within the coexistence region, with a maximum at the sintering temperature of 1150 °C. This agrees is well with the literature results explained on the basic of the mixing rules [16,17]. The increase of the piezoelectric properties is ascribed to the different spontaneous polarization directions from each phase. It has been reported that the amount of the domain within non-180° dipoles, which would contribute to the ionic coupling under polling, increased with the increase of the relative amount of the rhombohedral phase. Therefore, the value of k_p would increase with the appearance of small amount of rhombohedral phase in the coexistence region. However, the effect of the phase coexistence will decrease when the relative amount of rhombohedral phase is too small and the value of the k_p decreases.

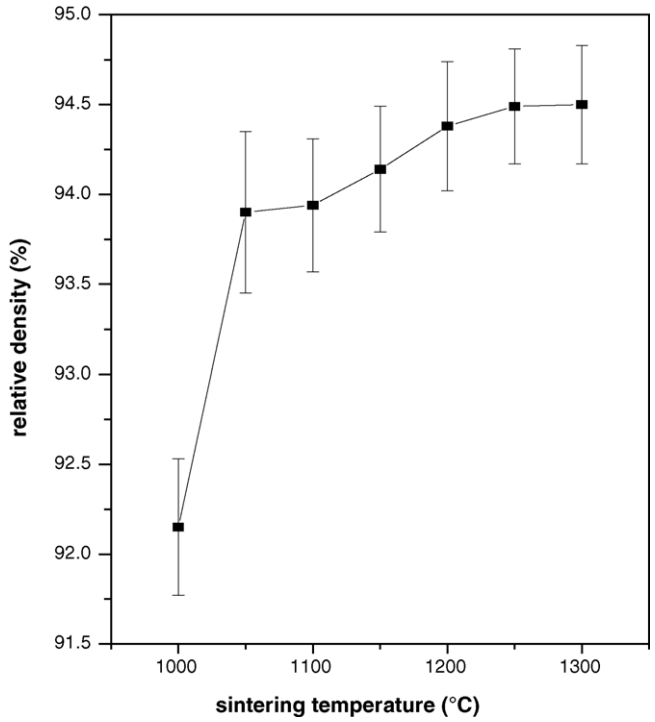

Fig. 6. Density (expressed as percent of 8.00 g/cm^3) as a function of sintering temperature.

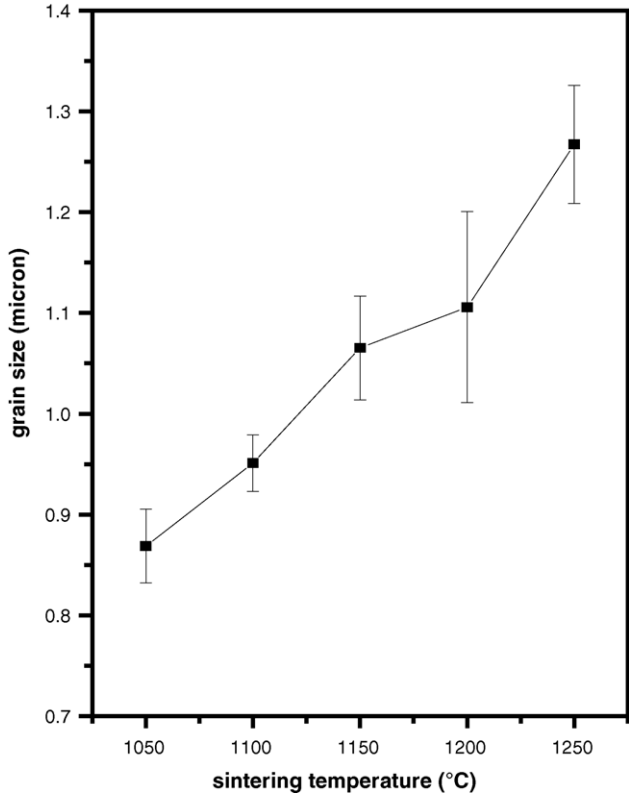

Fig. 7. Variation of the average grain size with the sintering temperatures.

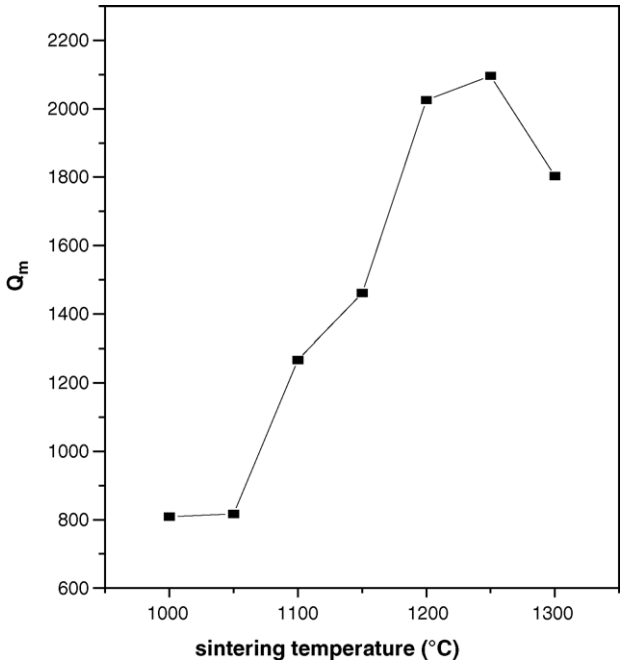

Fig. 8. Mechanical quality factor (Q_m) for the samples measured at different sintering temperatures.

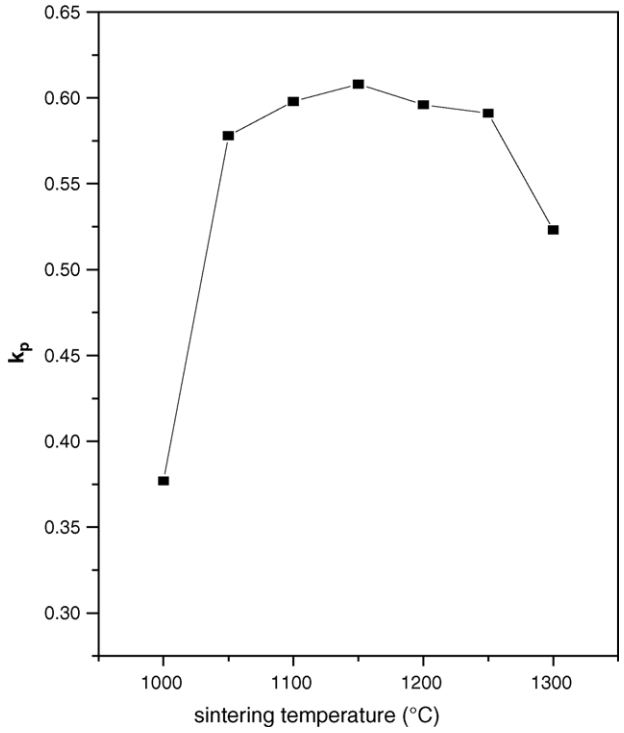

Fig. 9. Electromechanical planar coupling coefficient k_p for the samples sintered at different temperatures.

4. Conclusions

$0.07Pb(Mn_{1/3}Nb_{2/3})O_3$–$0.468PbZrO_3$–$0.462PbTiO_3$ piezoelectric ceramics were prepared through conventional mixed oxide route at various sintering temperature. It was found that the tetragonal/rhombohedral phase coexistence region occurs

in the sintering temperature range between 1050 and 1250 °C. The cell parameters a_T and c_T of the tetragonal phase decreased, whereas the parameter a_R of the rhombohedral phase increased as the sintering temperature increased in the phase coexistence region. The relative amount of the rhombohedral phase decreased as the sintering temperature increased. The value of Q_m of the sample increased as the sintering temperatures increased in the coexistence region. The k_p factor is higher in the coexistence region, its maximum value being measured at the sintering temperature of 1150 °C.

Acknowledgement

Financial support of this research by National Science Council, Taiwan, ROC, under the grant NSC 89-2218-E-036-017 is gratefully acknowledged.

References

[1] K.W. Tang, H.L.W. Chana, Y.M. Cheungb, P.C.K. Liu, Mater. Chem. Phys. 75 (2002) 196.
[2] E. Quandt, A. Ludwig, Sens. Actuators 81 (2000) 275.
[3] R. Zuo, L. Li, X. Hu, Z. Gui, Mater. Lett. 54 (2002) 185.
[4] K. Nagata, J. Thongrueng, J. Korea Appl. Soc. 32 (1998) S1278.
[5] A. Pinczuk, Solid State Commun. 12 (1973) 1035.
[6] K. Okazaki, K. Nagata, J. Am. Ceram. Soc. 56 (1973) 82.
[7] J.C. Fernandes, D.A. Hall, M.R. Cockburn, G.N. Greaves, Nucl. Instrum. Methods Phys. Res., B 98 (1995) 137.
[8] E.R. Nielsen, E. Ringgaard, M. Kosec, J. Eur. Ceram. Soc. 22 (2002) 1847.
[9] D.E. Wittmer, R.C. Buchanan, J. Am. Ceram. Soc. 64 (1981) 485.
[10] K. Murakami, D. Mabuchi, T. Kurita, Y. Niwa, S. Kaneko, Jpn. J. Appl. Phys. 35 (1996) 5188.
[11] M. Pereira, A.G. Peixoto, M.J.M. Gomes, J. Eur. Ceram. Soc. 21 (2001) 1353.
[12] J. Kim, K. Yoon, J. Mater. Sci. 29 (1994) 809.
[13] A.P. Barranco, F.C. Pinar, P. Martinez, E.T. Garcia, J. Eur. Ceram. Soc. 21 (2001) 523.
[14] C.-H. Chen, H.-L. Lin, Mater. Chem. Phys. (2006) in press.
[15] A. Boutarfaia, Ceram. Int. 26 (2000) 583.
[16] C.-H. Wang, J. Eur. Ceram. Soc. 22 (20022033).
[17] V.A. Isupov, Ferroelectrics 46 (1983) 217.
[18] R.D. Shannon, C.T. Previtt, Acta Crystallogr., B. 25 (1969) 925.